CHANGE DETECTION IN ALUMINUM ELECTRODE IMAGE DURING OHMIC HEATING USING PRINCIPAL COMPONENT ANALYSIS

Elvianto Dwi Hartono[1,2], Bagus Hardiansyah[2], Anang Lastriyanto[3], Elok Zubaidah[4], Yusuf Hendrawan[3]
[1] Department of Agroindustrial Technology, Faculty of Agricultural Technology
Universitas Brawijaya Malang, Malang 65145, Indonesia
[2] Department of Informatics Engineering, Faculty of Engineering
Universitas 17 Agustus 1945 Surabaya, Surabaya 60118, Indonesia
[3] Department of Biosystems Engineering, Faculty of Agricultural Technology
Universitas Brawijaya Malang, Malang 65145, Indonesia
[4] Department of Food Science and Technology, Faculty of Agricultural Technology
Universitas Brawijaya Malang, Malang 65145, Indonesia
elvianto.evh@untag-sby.ac.id

ABSTRAK

In this paper, we propose a novel technique for unsupervised change detection dataset derived from a process pasteurization using aluminium plate left and right with frequencies 1kHz, 2kHz, 100Hz, 250Hz images using principal component analysis (PCA) and k-means clustering. The distinct image is partitioned into h × h non-overlapping blocks. orthonormal eigenvectors are extracted through PCA of $h \times h$ non-overlapping block set to create an eigenvector space. Each pixel within the distinct image is characterized by a feature vector of a certain dimensionality. This feature vector is obtained projection the $h \times h$ distinct image data onto the eigenvector space that has been generated. Change detection is accomplished by dividing the feature vector space into two clusters through the application of k-means clustering with k=2. Each pixel is then assigned to one of these two clusters based on the minimum Euclidean distance between the pixel's feature vector and the mean feature vector of the clusters. Empirical results validate the effectiveness of the proposed approach.

Keyword : *Change detection, k-means clustering, principal component analysis, Aluminum Electrode*

1. INTRODUCTION

Change detection techniques can be divided into two main categories: supervised and unsupervised, depending on how data processing is performed. The supervised method involves using a supervised classification approach, which relies on having a ground truth to create an appropriate training set for classifiers. On the other hand, unsupervised method for change detection involves directly comparing two multi-temporal images without incorporating any additional data.

Change detection methods primarily rely on the automated analysis of change data derived from multi-temporal images. These data are produced using one of the following techniques: Image differencing, Normalized difference vegetation index, Change vector analysis, Principal Component Analysis (PCA), and Image rationing [1].

In the literature, numerous unsupervised change detection methods have been proposed within these categories, utilizing intricate data modeling and parameter estimation techniques. [2], [3]. The majority of unsupervised change detection methods rely on the image differencing technique. These algorithms achieve change detection by subtracting the pixel values of two images acquired at different time instances, resulting in a new image called the distinct image. The distinct image consists of pixels that represent cover area or changes area, displaying values notably distinct from those found in unaltered regions. Changes are subsequently identified through an analysis of this distinct image.

Two automated methods rooted in Bayesian theory are suggested for analyzing the distinct image [4]: Expectation - Maximization (EM) - based thresholding: This technique allows for an automatic selection of the decision threshold, aiming to maximize the overall change detection accuracy. It assumes spatial independence of pixels in the distinct image. Markov Random Fields (MRF)-based thresholding: This approach considers spatial contextual information from the neighborhood of each pixel in the distinct image. By exploiting the context of interpixel class dependence within Markov random fields, it enhances change detection performance. However, it's crucial to acknowledge that the MRF-based thresholding algorithm requires significant computational resources, rendering it unsuitable for near real-time change detection applications. Moreover, several other change detection techniques adopt a similar framework for synthetic aperture radar (SAR) images, achieving commendable outcomes through the utilization of intricate data modeling and parameter estimation methods. Nevertheless, these approaches encounter the challenge of speckle noise inference when applied to the raw data domain.

An essential concept ohmic heating is Ohm’s Law, where voltage and flow are directed directly to a conductor, which is described as resistance [5]. Furthermore, ohmic heating depends on volumetric heating, needs high performance, and converts electrical power into heat energy [6]. The application of ohmic heating to food products has widely replaced the pasteurization process. In ohmic heating, there is a connection between two conductors, solid-state and liquid-state, which are connected to an alternating current source due to the joule effect [7].

The implementation of computer vision, which is based on the evaluation of agriculture and food goods, obviously encountered many challenges, necessitating the need for such a precise, quick, and impartial method to assess the caliber of the evaluated material [8]. Furthermore, the method creates automated equipment for the food and agricultural sectors. Computer vision development is based on the inspection of food quality and agricultural products, which unfortunately faced several obstacles that later required such an efficient, accurate, fast, and objective technique in determining the quality of the measured material. In this study, the honey image dataset derived from a process pasteurization using aluminium plate left and right with frequencies 1kHz, 2kHz, 100Hz, 250Hz.

This letter introduces a computationally straightforward yet remarkably efficient automatic change detection approach. The suggested method entails the examination of the distinct image obtained from two aluminium plate images taken over the identical area but at two distinct time points. In this approach, the distinct image is divided into non-overlapping blocks. Each of these blocks is used to extract eigenvectors using Principal Component Analysis (PCA) [9]. Feature vector is derived for each pixel in the distinct image. This is achieved by projecting the data from its $h \times h$ neighborhood onto the eigenvector space obtained through the PCA process. In the final step of the change detection process, the feature vector space is partitioned into two clusters using the k-means algorithm, and each cluster is characterized by a mean feature vector. To detect changes, each pixel in the distinct image is assigned to one of the clusters based on the minimum Euclidean distance between its feature vector and the mean feature vectors of the clusters. Every pixel in the distinct image is classified as either belonging to the "change" cluster or the "unchanged" cluster, thus achieving the change detection outcome.

This letter is organized into three sections. Section II provides an in-depth explanation of the proposed change detection with unsupervised method. Section III show cases the experimental outcomes of the proposed approach, encompassing noisy images. Lastly, Section IV serves as the conclusion, summarizing the study's findings and contributions.

Figure 1. Aluminium Plate Process the Ohmic Heating of Honey

2. CHANGE DETECTION METHOD

Let's contemplate two intensity images, denoted as X_1 and X_2, both captured over the identical area but at distinct time instances: t_1 and t_2, respectively. Our goal is to produce a change detection map, commonly referred to as a change map, which visually portrays alterations that have transpired on the surface between the moments of capturing the two images, X_1 and X_2. The task of change detection can be conceptualized as a binary classification challenge. Let changed (denoted by w_c) and unchanged (denoted by w_u) pixels on the images X_1 and X_2 be the set of classes. Let w_c and w_u represent the classes corresponding to changed (w_c) and unchanged (w_u) pixels within the images X_1 and X_2.

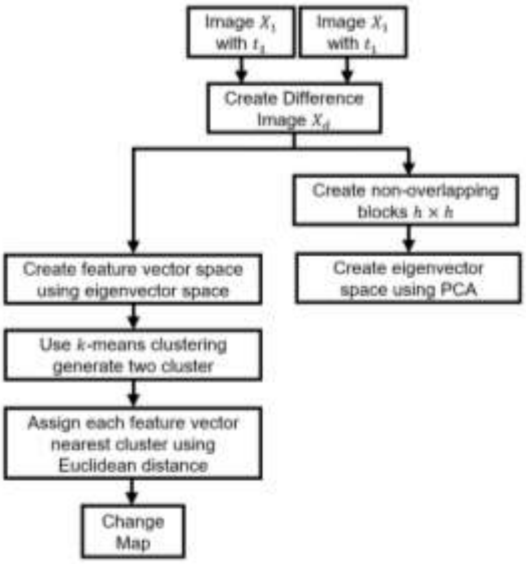

Figure 2. General Framework Change Map Detection Approach

The proposed approach encompasses six main steps, as depicted in Figure 1:

1. Creation of the distinct image.
2. Creation non-overlapping blocks with dimensions $h \times h$ from the distinct image.
3. Formation of an eigenvector by applying PCA to the non-overlapping image blocks of size $h \times h$.
4. Formation of a feature vector space across the entire distinct image is achieved by projecting overlapping blocks with dimensions $h \times h$ around each pixel onto the eigenvector space.

5. Feature vector space two clusters, connected to w_c and w_u, utilizing the k-means algorithm with $k = 2$.
6. Change map by linking each pixel in the distinct image with one of the clusters, determined by the minimum Euclidean distance between its feature vector and the mean feature vector of the clusters.

The initial phase of the suggested algorithm involves the creation of the distinct image. Let X_d denote this distinct image, which can be defined in varying ways depending on the nature of the input image. In the case of optical images, X_d can be defined as the absolute difference between the intensity values of the two images.

$$X_d = |X_2 - X_1| \qquad (1)$$

The second phase of the proposed method involves dividing X_d into non-overlapping blocks with dimensions $h \times h$. We denote the $h \times h$ difference-image block at coordinates (y, x) (centered at (y, x) when h is odd) as $X_d\ (y, x)$. Here, the operator is a mathematical ceiling function that rounds a number up to the nearest integer. By applying lexicographical ordering to $X_d\ (y, x)$, we can derive a vector representation.

$$X_d(x, y) = \left[X_d\left(y - \left\lceil\frac{h}{2}\right\rceil + 1, x - \left\lceil\frac{h}{2}\right\rceil + 1\right) X_d\left(y + h - \left\lceil\frac{h}{2}\right\rceil, x - \left\lceil\frac{h}{2}\right\rceil + 1\right)\right] \qquad (2)$$

The set of vectors $x_d(y, x)$ is employed to construct an eigenvector space through Principal Component Analysis (PCA) [9]. For ease of mathematical notation, we utilize x_d^p to represent the vector $x_d(y, x)$, where the operator signifies the mathematical function that a number to the nearest. The vector of set is defined by

$$\psi = \frac{1}{M}\sum_{P=1}^{M} \quad x_d^p \qquad (3)$$

Each vector varies from the average vector due to the vector δ. Utilizing Principal Component Analysis (PCA), a collection of N orthonormal vectors e_s and their corresponding scalars λ_s is sought to effectively capture the data distribution. This process is employed on the set of difference vectors denoted as δ_p. The vectors e_s and their corresponding scalars λ_s correspond to the eigenvectors and eigenvalues of the covariance matrix [10], respectively.

$$C = \frac{1}{M}\sum_{P=1}^{M} \quad \delta_p \delta_p^T \qquad (4)$$

Corresponding to the transpose of the vector δ_p^T, the matrix C has dimensions of $h^2 \times h^2$, contributing to the determination of h^2 eigenvectors and their corresponding eigenvalues. Let's suppose that the eigenvectors generated from matrix C are arranged in a descending order based on their eigenvalues.

$$V(i, j) = [v_1, v_2 \cdots v_n]^T \qquad (5)$$

The feature vector constructed by projecting $x_d(i, j)$ onto the eigenvector each pixel located coordinates (i, j). The parameter S defines the dimension of the feature vector $V(i, j)$ at spatial coordinates (i, j). It corresponds to the number of eigenvectors utilized in the projection of $x_d(i, j)$ onto the eigenvector space.

The next step in the proposed method involves the formation of two clusters via the application of the k-means clustering algorithm $k = 2$ within the feature vector space. In this case, the value of k is set to 2. Let V_{w_u} and V_{w_c} represent the cluster mean feature vectors corresponding to classes w_u and w_c, respectively. To assign labels to the clusters generated by the k-means clustering algorithm, the labeled pixels obtained from this method are utilized calculate two average values across the entirety of the distinct image. Given the expectation that regions displaying changes between the two images tend to have higher distinct image pixel values in those areas compared to regions without changes, a deduction can be made. This assumption guides the assignment of labels to the clusters: the cluster with pixels possessing a reduce the average value in the distinct image is designated as the w_u, while the other clustering is assigned as the w_c class.

A binary change map (CM) is generated using V_{w_u} and V_{w_c}. In this map, a value of "1" signifies the corresponding pixel position indicates a change to the w_c class, while a value of "0" indicates no change and pertains to the w_u class.

$$CM(i, j) = \{1, 0, \|V(i, j) - V_{w_c}\|_2^2 \leq \|V(i, j) - V_{w_u}\|_2^2\ otherwise \qquad (6)$$

Where $\|\|_2^2$ is Euclidean distance.

3. EXPERIMENTAL RESULTS

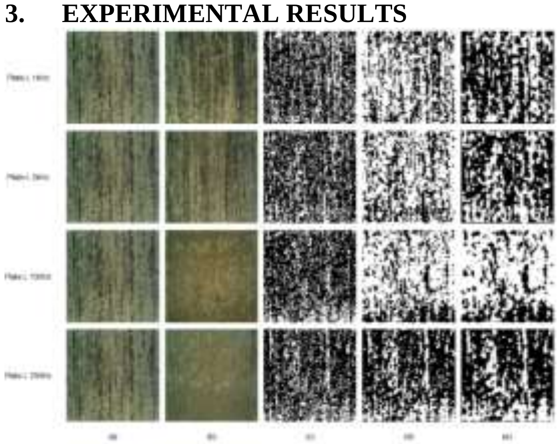

Figure 3. Qualitative Results: Change detection results for various methods applied to optical

images captured from the Left Plate Aluminium. (a) Input image X1. (b) Input image X2. (c) EM-based thresholding [4]. (d) MRF-based thresholding with β = 1.6 [4]. (e) Proposed approach.

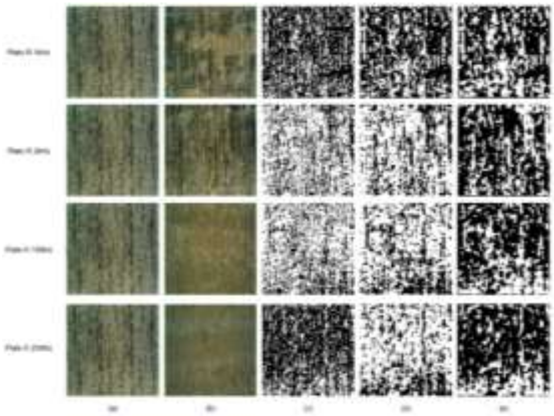

Figure 4. Qualitative Results: Change detection results for various methods applied to optical images captured from the Right Plate Aluminium. (a) Input image X1. (b) Input image X2. (c) EM-based thresholding [4]. (d) MRF-based thresholding with β = 1.6 [4]. (e) Proposed approach.

To evaluate the performance of the proposed method, we utilized a primary dataset containing both left and right aluminium plate images. This dataset encompasses a range of optical images, as illustrated in Figure 3 and Figure 4. We conducted validation qualitative and quantitative comparisons with the methods outlined [4]. The method detailed in [4] were Applied identical parameter settings as those presented in this letter. Two techniques proposed in [4] for analyzing the distinct image and generating change map were considered: EM-based thresholding MRF-based thresholding The first approach is parameter-free, while the second approach depends on a parameter β that regulates the impact of spatial contextual information on the change detection process. For this study, we opted to use $\beta = 1.6$ as specified in [11]–[13].

During the experiments, the values chosen were $h = 4$ and $S = 3$. Within each $h \times h$ block of the distinct image, three different types of data from the distinct image could be present: 1) No-change data; 2) Change data; 3) Mixture of change and no-change data. The first two scenarios arise when the $h \times h$ block is fully situated within either the changed or unchanged regions of the distinct image. The third scenario occurs when the $h \times h$ block is positioned along the boundaries between areas of change and areas without change in the distinct image [14]–[16]. Thus, each of these data types can be represented using an eigenvector, indicating that $S = 3$. It's important to note that we conducted a comprehensive set of experiments where $3 < S \leq h^2$, and these experiments revealed that there was no significant alteration in the change detection performance in comparison to the case of $S = 3$.

As depicted in Figures 3 and 4 (c)–(e), it's evident that the resulting change maps accurately represent the alterations within the identical surface area of the aluminium plate. Qualitative results shown in Figure 3, Figure 4 that EM-based thresholding in Figure 3, Figure 4 (c) the highest rate of false detections. The false detections reduced through of MRF-based contextual details in Figure 3, Figure 4 (d). Increased values of β lead to reduced false detections, but at the cost of higher missed detections. The outcome of the suggested method is displayed in Figure. 3(e) left plate aluminium, Figure. 4(e) right plate aluminium and provides better qualitative results with respect to the other approaches.

In the process of acquiring images, it's common to encounter various forms of noise [17], [18]. Hence, it's intriguing to assess how well the proposed automatic change detection method can handle different types of noise interference. Various levels and types of noise are intentionally introduced into the input image. This is depicted in Figure 3 and Figure 4(a), offering insights into the method's effectiveness in addressing diverse noise challenges.

3.1. QUANTITATIVE QUALITY MEASUREMENTS

In this research, we used quality performance in the experiment, i.e., the root mean square error (RMSE) [19], [20]. The root-mean-squared error (RMSE) are standard metrics used in model evaluation. For a sample of n observations $y = (y_i, i = 1,2, \dots, n)$ and n corresponding model predictions. In experiment, it is typically necessary to obtain a single comprehensive quality assessment for the entire image. We use a mean RMSE Mean Root Mean Squared Error (MRMSE) to validation the image quality from single image:

$$MRMSE(X,Y) = \frac{1}{n}\sum_{i=1}^{n} \quad \|x_i - y_i\|_2^2 \qquad (7)$$

Here, X represents the reference image, while Y corresponds to the distorted image. Additionally, x_i and y_i denote the image contents within the $i-th$ local window, and, n for the total count of local windows image. Depending on the specific application, it is feasible to calculate a weighted average of various samples in the RMSE index change map. Another illustration involves the observation that diverse image textures tend to capture human attention to varying extents. A smoothly transitioning foveated weighting model could be utilized to establish these weights. However, in this paper, we adopt a uniform weighting approach. We also provide a MATLAB implementation of the RMSE index algorithm.

4. BEST-CASE/WORST-CASE VALIDATION RESULTS

Several image quality assessment algorithms have demonstrated consistent behavior when applied to distorted images generated from a single original image, employing the same type of distortions. However, the efficiency of these models noticeably declines when utilized on a collection of images stemming from diverse reference images and/or encompassing a range of distinct types of distortions. We also have developed a more efficient methodology for examining the relationship between our objective measure and perceived quality. Starting from a distorted image, we ascend/descend the gradient of MRMSE while constraining the RMSE to remain equal to that of the initial distorted image. To experiment the effectiveness we report some visual results of the Figure 3, and 4, According to the results tabulated in Table 1 Quantitative Performance of image quality assessment models. CC: correlation coefficient MRMS: mean root mean squared error. In this experiment we using devide three parameter for better result validation. The best result quantitative validation in block size H=6 and the worst walidation in block size H=2, in this case we using primary dataset for process pasteurization using aluminium plate left and right with frequencies 1kHz, 2kHz, 100Hz, 250Hz images.

Table 1. Quantitative Performance of image quality assessment models. Correlation Coefficient (CC); Mean Root Mean Squared Error MRMS

Dataset	MRMSE		
	Block Size H=2	**Block Size H=4**	**Block Size H=6**
Plate Left 1kHz	0.1033	0.0069	0.0072
Plate Left 2kHz	0.1004	0.0087	0.0068
Plate Left 100Hz	0.0964	0.1430	0.1425
Plate Left 250Hz	0.0968	0.0996	0.1017
Plate Right 1kHz	0.0995	0.1042	0.0068
Plate Right 2kHz	0.1427	0.1425	0.1027
Plate Right 100Hz	0.1427	0.1410	0.1051
Plate Right 250Hz	0.0981	0.1440	0.0966

5. CONCLUSION

This article presents an unsupervised change detection method that utilizes k-means clustering on feature vectors. The feature vectors are obtained by projecting local data of size $h \times h$ onto the eigenvector space, which is constructed through Principal Component Analysis (PCA) on non-overlapping image blocks of size $h \times h$. The proposed technique extracts the feature vector for each pixel by considering a neighborhood of size $h \times h$. This approach inherently incorporates contextual information. The proposed algorithm strikes a balance between computational simplicity and effective identification of significant changes, rendering it well-suited for real-time applications. The results requires computationally expensive data modeling and parameter estimation. Simulation results show that the proposed algorithm performs quite well on combating both the zero-mean Gaussian noise and the speckle noise, which is quite attractive for change detection in optical and primary dataset in aluminium plate survace images area.

REFERENCE

[1] F. Pacirici, C. Solimini, F. Del Frate, and W. J. Emery, "An innovative neural-net method to detect temporal changes in high-resolution optical satellite imagery," *IEEE Trans. Geosci. Remote Sens.*, vol. 45, no. 9, pp. 2940–2952, 2007, doi: 10.1109/TGRS.2007.902824.

[2] F. Bovolo, L. Bruzzone, and S. Member, "A Split-Based Approach to Unsupervised Change Detection in Large-Size Multitemporal Images : Application to Tsunami-Damage Assessment," vol. 45, no. 6, pp. 1658–1670, 2007.

[3] F. Bovolo, L. Bruzzone, and S. Member, "A Novel Approach to Unsupervised Change Detection Based on a Semisupervised SVM and a Similarity Measure," vol. 46, no. 7, pp. 2070–2082, 2008.

[4] L. Bruzzone and S. Member, "Unsupervised Change Detection," vol. 38, no. 3, pp. 1171–1182, 2000.

[5] Z. T. Alkanan, A. B. Altemimi, A. R. S. Al-Hilphy, D. G. Watson, and A. Pratap-Singh, "Ohmic heating in the food industry: Developments in concepts and applications during 2013–2020," *Appl. Sci.*, vol. 11, no. 6, 2021, doi: 10.3390/app11062507.

[6] S. H. Park, V. M. Balasubramaniam, S. K. Sastry, and J. Lee, "Pressure-ohmic-thermal sterilization: A feasible approach for the inactivation of Bacillus amyloliquefaciens and Geobacillus stearothermophilus spores," *Innov. Food Sci. Emerg. Technol.*, vol. 19, no. 2013, pp. 115–123, 2013, doi: 10.1016/j.ifset.2013.03.005.

[7] H. A. Makroo, N. K. Rastogi, and B. Srivastava, "Ohmic heating assisted inactivation of enzymes and microorganisms in foods: A review," *Trends Food Sci. Technol.*, vol. 97, no. January 2019, pp. 451–465, 2020, doi: 10.1016/j.tifs.2020.01.015.

[8] K. K. Patel, A. Kar, S. N. Jha, and M. A. Khan, "Machine vision system: A tool for quality inspection of food and agricultural products," *J. Food Sci. Technol.*, vol. 49, no. 2, pp. 123–

141, 2012, doi: 10.1007/s13197-011-0321-4.

[9] B. Hardiansyah and Y. Lu, "Single image super-resolution via multiple linear mapping anchored neighborhood regression," *Multimed. Tools Appl.*, vol. 80, no. 19, pp. 28713–28730, 2021, doi: 10.1007/s11042-021-11062-0.

[10] R. Herteno, D. Kartini, I. Budiman, I. Komputer, F. Matematika dan Ilmu Pengetahuan Alam, and U. Lambung Mangkurat Banjarbaru, "Implementasi Metode Principal Component Analysis (Pca) Dan Modified K-Nearest Neighbor Pada Klasifikasi Citra Daun Tanaman Herbal," *J. Mnemon.*, vol. 6, no. 2, pp. 1–9, 2023.

[11] G.-H. Wang, B.-B. Gao, and C. Wang, "How to Reduce Change Detection to Semantic Segmentation," *Pattern Recognit.*, vol. 138, p. 109384, 2023.

[12] C. JST, "Change detection from a street image pair using cnn features and superpixel segmentation," 2015.

[13] Y. Wang *et al.*, "Mask DeepLab: End-to-end image segmentation for change detection in high-resolution remote sensing images," *Int. J. Appl. Earth Obs. Geoinf.*, vol. 104, p. 102582, 2021.

[14] Y. Yu, Y. Shen, Y. Liu, Y. Wei, X. Rui, and B. Li, "Knowledge mapping and trends in research on remote sensing change detection using CiteSpace analysis," *Earth Sci. Informatics*, vol. 16, no. 1, pp. 787–801, 2023.

[15] S. Liang, Z. Hua, and J. Li, "Hybrid transformer-CNN networks using superpixel segmentation for remote sensing building change detection," *Int. J. Remote Sens.*, vol. 44, no. 8, pp. 2754–2780, 2023.

[16] C. Wu, B. Du, and L. Zhang, "Fully convolutional change detection framework with generative adversarial network for unsupervised, weakly supervised and regional supervised change detection," *IEEE Trans. Pattern Anal. Mach. Intell.*, 2023.

[17] T. Bai *et al.*, "Deep learning for change detection in remote sensing: a review," *Geo-spatial Inf. Sci.*, vol. 26, no. 3, pp. 262–288, 2023.

[18] Y. Deng, Y. Meng, J. Chen, A. Yue, D. Liu, and J. Chen, "TChange: A Hybrid Transformer-CNN Change Detection Network," *Remote Sens.*, vol. 15, no. 5, p. 1219, 2023.

[19] S. Sahu, "Comparative Analysis of Image Enhancement Techniques for Ultrasound Liver Image," *Int. J. Electr. Comput. Eng.*, vol. 2, no. 6, pp. 792–797, 2012, doi: 10.11591/ijece.v2i6.1513.

[20] J. Im, J. R. Jensen, and J. A. Tullis, "Object-based change detection using correlation image analysis and image segmentation," *Int. J. Remote Sens.*, vol. 29, no. 2, pp. 399–423, 2008.